NPS-EC-95-009

NAVAL POSTGRADUATE SCHOOL
Monterey, California

BEAM MOTION INDUCED DOPPLER SHIFT OF AN EXTENDED OBJECT

by

Hung-Mou Lee

October 1995

Approved for public release; distribution is unlimited.

Prepared for: Program Executive Office, Theater Air Defense
2531 Jefferson Davis Highway
Arlington, VA 22242-5170

Naval Postgraduate School
Monterey, California 93943-5000

Rear Admiral Marsha J. Evans
Superintendent

Richard E. Elster
Provost

This report was sponsored by the Program Executive Office, Theater Air Defense.

Approved for public release; distribution unlimited.

This report was prepared by:

Hung-Mou Lee
Associate Professor of Electrical
and Computer Engineering

Reviewed by:

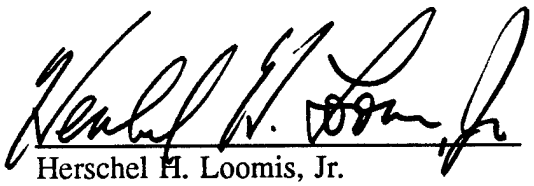

Herschel H. Loomis, Jr.
Chairman
Department of Electrical
and Computer Engineering

Released by:

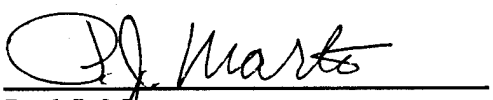

Paul J. Marto
Dean of Research

REPORT DOCUMENTATION PAGE

Form Approved
OMB No. 0704-0188

1. AGENCY USE ONLY (Leave blank)	2. REPORT DATE	3. REPORT TYPE AND DATES COVERED
	October 1995	Final Report 1 Oct 1994–30 Sep 1995

4. TITLE AND SUBTITLE
Beam Motion Induced Doppler Shift of an Extended Object

5. FUNDING NUMBERS
N0002495WRD0164

6. AUTHOR(S)
Hung-Mou Lee

7. PERFORMING ORGANIZATION NAME(S) AND ADDRESS(ES)
Naval Postgraduate School
Monterey, CA 93943-5000

8. PERFORMING ORGANIZATION REPORT NUMBER
NPSEC-95-009

9. SPONSORING / MONITORING AGENCY NAME(S) AND ADDRESS(ES)
Program Executive Office
Theater Air Defense
2531 Jefferson Davis Highway
Arlington, VA 22242-5170

10. SPONSORING / MONITORING AGENCY REPORT NUMBER

11. SUPPLEMENTARY NOTES
The views expressed in this report are those of the authors and do not reflect the official policy or position of the Department of Defense or the United States Government.

12a. DISTRIBUTION / AVAILABILITY STATEMENT
Approved for public release; distribution unlimited.

12b. DISTRIBUTION CODE

13. ABSTRACT *(Maximum 200 words)*

A technique to synthesize radar echo on a pulse-to-pulse basis is introduced. It is applied to the analysis of ground reflections where an extended object is present. Since the extended object reflects the radar illumination in a regular manner from pulse to pulse, it introduces phase shifts into the echoes and makes the echoes appear to come from high speed target. The impacts of this phenomenon on the performance of systems which rely on Doppler filtering should be assessed in the future. Furthermore, since this phenomenon is expected to occur when slow moving extended objects such as sea swells are present in short ranges, it is important to take this phenomenon into consideration when weapon systems for ship self-defense are deployed.

14. SUBJECT TERMS	15. NUMBER OF PAGES
radar, littoral region, echo, Doppler shift and filtering, pulse-increment cells	41
	16. PRICE CODE

17. SECURITY CLASSIFICATION OF REPORT	18. SECURITY CLASSIFICATION OF THIS PAGE	19. SECURITY CLASSIFICATION OF ABSTRACT	20. LIMITATION OF ABSTRACT
UNCLASSIFIED	UNCLASSIFIED	UNCLASSIFIED	SAR

ABSTRACT

A technique to synthesize radar echo on a pulse-to-pulse basis is introduced. It is applied to the analysis of ground reflections where an extended object is present. Since the extended object reflects the radar illumination in a regular manner from pulse to pulse, it introduces phase shifts into the echoes and makes the echoes appear to come from high speed target. The impacts of this phenomenon on the performance of systems which rely on Doppler filtering should be assessed in the future. Furthermore, since this phenomenon is expected to occur when slow moving extended objects such as sea swells are present in short ranges, it is important to take this phenomenon into consideration when weapon systems for ship self-defense are deployed.

TABLE OF CONTENTS

I. INTRODUCTION

1. The Scope

Doppler processing makes use of the pulse-to-pulse phase change of radar echoes produced by a moving object to differentiate a fast approaching target from a slow one [1]. To give an accurate description of the echoes, pulse-to-pulse changes over the radar footprint must be included in the consideration. There are two sources which contribute to the changes in two consecutive echoes when the beam is moving: first of all, the illuminated regions are different; then, on the overlapping portion of the regions, the radar illuminates it differently from pulse to pulse. To show that drastic effects can occur when a radar beam is moving, the oversimplifying situation of a radar transmitting a narrow beam of uniform strength which bounces off an extended object is considered in this chapter. The phases of the returned signals are changing steadily and significantly from pulse to pulse, causing the Doppler filter to classify the object as moving.

One of the purposes of this study is to establish a framework for synthesizing the returned signal of a radar transmission in a complicated operating environment when the beam is moving. To this end, the technique of generating the "pulse-increment composite echo" is introduced in Chapter II: For a scanning radar, the change in beam angle between pulses determines the angular size of the pulse-increment cells which are bounded between two consecutive range gates. The region of interest is covered with these pulse-increment cells and environmental information within each cell is digitized for estimated radar reflectivity. As the radar beam scans, the antenna

gain and phase shift for each pulse-increment cell under the radar footprint are combined with the digitized reflectivity to produce the radar echo. These procedures can be modified for tracking radars whose beam motions are more agile but nonetheless are limited by their servo bandwidths. In short range situations when the strength of the returned signal is not in question such as ship defense in the littoral region or missile terminal homing towards its surface skimming prey, such a framework is all what it requires to bridge the gap between a well-modeled transmitter-receiver pair in studying the performance of a radar.

As a demonstration, this technique is applied to a generic 2D search radar with a Gaussian mainbeam scanning over the same type of extended object discussed later in this chapter. The composite echoes are processed using a six-pulse fast Fourier transform (FFT) Doppler filter bank. Signals from the three higher speed channels are reduced into one output pulse in two ways: collapse them into one by selecting only the signal of the greatest strength [2] or sum them together coherently. The phases of two consecutive pulses are then compared to deduce the apparent velocity of the extended object.

It is clear from this study that, due to the pulse-to-pulse changes in radar echoes, a stationary or slowly moving extended object can appear to be fast moving and affect both the search and the tracking functions of radars as long as Doppler processing remains an indispensable tool for singling out the moving target of interest from other targets and from background clutter. How a shoreline in the immediate foreground impacts on the firing of the Phalanx and whether a sea swell will cause a SeaSparrow to plunge into the ocean in the final few seconds cannot be answered without looking closely into the actual workings of the specific signal receiving and processing units.

2. Beam Motion Induced Doppler Shift

In the littoral region, there are many extended bodies whose shapes do not change significantly over their expanses: cliffs and ridges, stretches of plants and ground covers, streets and buildings. They are stationary, but in close range some of them may extend beyond a radar beamwidth (Table 1). For simplicity, the radar is assumed to transmit a beam which has a constant strength over its beamwidth and nothing outside. From pulse to pulse, if the radar beam is moving, the phases of the echoes from any of such extended objects can vary drastically because they are bouncing back from different portions of the extended object which are at different ranges from the radar. Thus, to the Doppler filter, the stationary extended object will appear to be moving. The condition under which such a phenomenon will arise is depicted in Figure 1.

Table 1. Footprint widths at close ranges for a radar of 3.3° beamwidth.

range (km)	2	10	25	50
footprint width (m)	115.2	576.0	1440	2880

The apparent speed of an extended object can be extremely high. It depends on the range, the speed of angular motion of the scanning or tracking radar beam, and the orientation of the object. The range vector of the radar beam and the direction of its angular motion define a plane in space which will be called the beam motion plane. In the beam motion plane, the normal to the running direction of the extended object makes an angle ψ with the radar beam as shown in

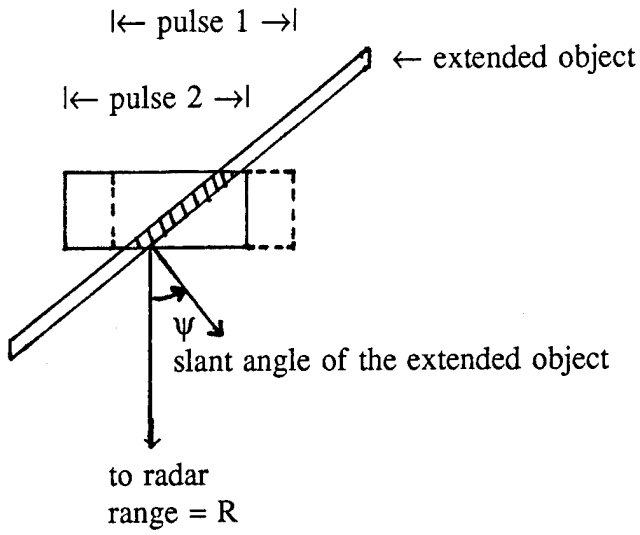

(a)

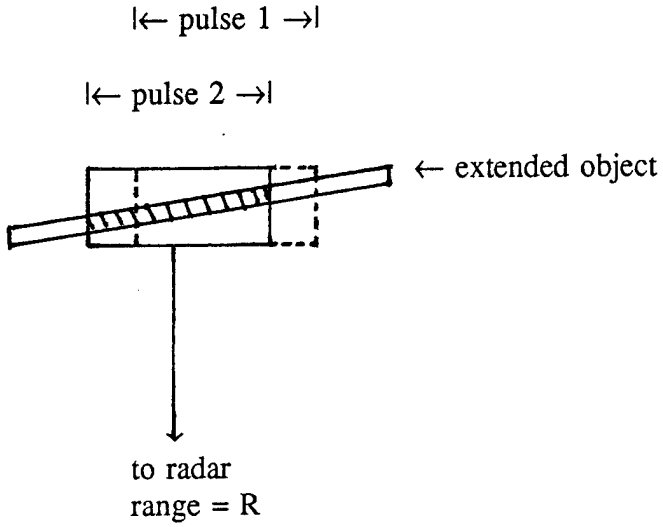

(b)

Figure 1. An object extends beyond a radar footprint on a range cell. Over two consecutive pulses, (a) the object appears stationary; (b) the object appears to have moved closer.

Fig. 1 (a). This angle will be called the slant angle. If the angular speed of beam motion is ω, which for a 2D search radar is $2\pi f_s$ with f_s measured in rotations (or cycles) per second, and if the range is denoted by R, then the apparent Doppler speed is $v_d = R\omega \tan\psi$. Table 2 shows this apparent speed of an extended object at a slant angle of 1° at various ranges. The radar is assumed to be scanning at 12 rpm, equivalent to an f_s of 0.2 cycles per second (Hz).

Table 2. Apparent doppler speed of an extended object slanted at 1° when a search radar is scanning at 12 rpm. The mach number assumes a speed of sound of 331 m/s.

range (km)	2	10	25	50
v_d (m/s)	43.87	219.3	548.4	1097
v_d (mach)	0.1325	0.6627	1.657	3.313

As can be seen from Fig. 1, the size of a range cell and the width of the radar footprint over the cell limit the maximum slant angle ψ_{max} of an extended object from which an apparent Doppler velocity can be observed. Since the apparent velocity is an increasing function of the slant angle, this maximum angle also serves to place an upper bound on the Doppler speed. For a pulse of duration τ, the size of a range cell is $c\tau/2$ where c is the speed of light. Since the width of the radar footprint is $R\theta_B$, where θ_B is the radar beamwidth, $\tan\psi_{max} = c\tau/(2R\theta_B)$. The maximum slant angles of an extended object to produce a Doppler shift to a radar having a 3.3° beamwidth and 2 μs pulse width at different ranges are given in Table 3. It should be noted that, at closer range, the same group of extended objects produces lower Doppler shifts with a smaller velocity spread than when they are farther away from the radar.

The maximum slant angle at each range translates into a maximum possible apparent velocity of $v_{max} = \omega c\tau/(2\theta_B)$ for a radar, which turns out to be independent of the range. For the radar considered in Tables 3, the apparent velocity from an extended object may vary from zero to a maximum equal to 6.55 km/s, or 19.8 mach. In addition to the introduction of false alarms in the Doppler channels of interest, signals containing Doppler shifts of up to such a high speed will produce Doppler fold-over which could be difficult to remove even with the use of multiple pulse repetition frequencies.

Table 3. Maximum slant angles of an extended object to produce a doppler speed at a radar of 3.3° beamwidth and 2μs pulse width.

range (km)	2	10	25	50
ψ_{max} (degrees)	69.0	27.5	11.8	5.95

The estimates above are legitimate but crude. A radar beam does not maintain a constant strength over its beamwidth and then falls to zero right outside of it. Therefore the maximum slant angle is not an absolute cutoff point beyond which an extended object shows no apparent velocity. The effects of the radar pulse width and its associated range cell size are even more complicated when pulse compression is utilized to generate the range gates: the uncompressed pulse typically covers a much deeper range cell which allows a greater ψ_{max}. The particular method with which pulse compression is performed determines the amplitudes and bandwidths of the signals fed into the Doppler filter and radar detector. A system-by-system analysis is required to evaluate the performance of each radar system operating under such an environment.

II. MOVING TARGET CHANNEL RESPONSE

1. Introduction

To investigate the phenomenon of beam motion induced Doppler shift of an extended object under a more realistic setting, a 2D search radar operating at 900 MHz and scanning at 12 rotations per minute (rpm) is considered. It is assumed that the radar has a pulse repetition frequency (PRF) of 1 kHz and utilizes a six-pulse fast Fourier transform (FFT) Doppler filter bank. For the radar footprint, the range cell is set at 300 m (about 2 μs pulse width) and the antenna is given a Gaussian shape mainbeam with a 3.3° half-power beamwidth θ_B and a sidelobe level of −30 dB below the peak.

Consider the operation of this radar in a coastal region having a smooth rolling terrain and a stretch of highway 10 kilometers from the radar as shown in Fig. 2(a). The radar echoes contain returns from the terrain, which can be assumed to exhibit a narrow Gaussian velocity spectrum, and returns from the highway. Over any range cell, as shown in Fig. 2(b), the radar footprint advances by an angle $\Delta\theta = 360\, f_s / f_p = 0.0720°$ from pulse to pulse. A new region within a range cell covered by this advancement of radar footprint will be called a pulse-increment cell. In fact, over a range cell, the radar footprint at any time can be considered as consisting of a chain of a fixed number of pulse-increment cells. As the radar scans, from pulse to pulse one pulse-increment cell is added from the advancing direction of the beam while another is dropped from the receding end. The radar echo of each transmitted pulse is thus the sum of returns from the pulse-increment cells under the instantaneous radar footprint.

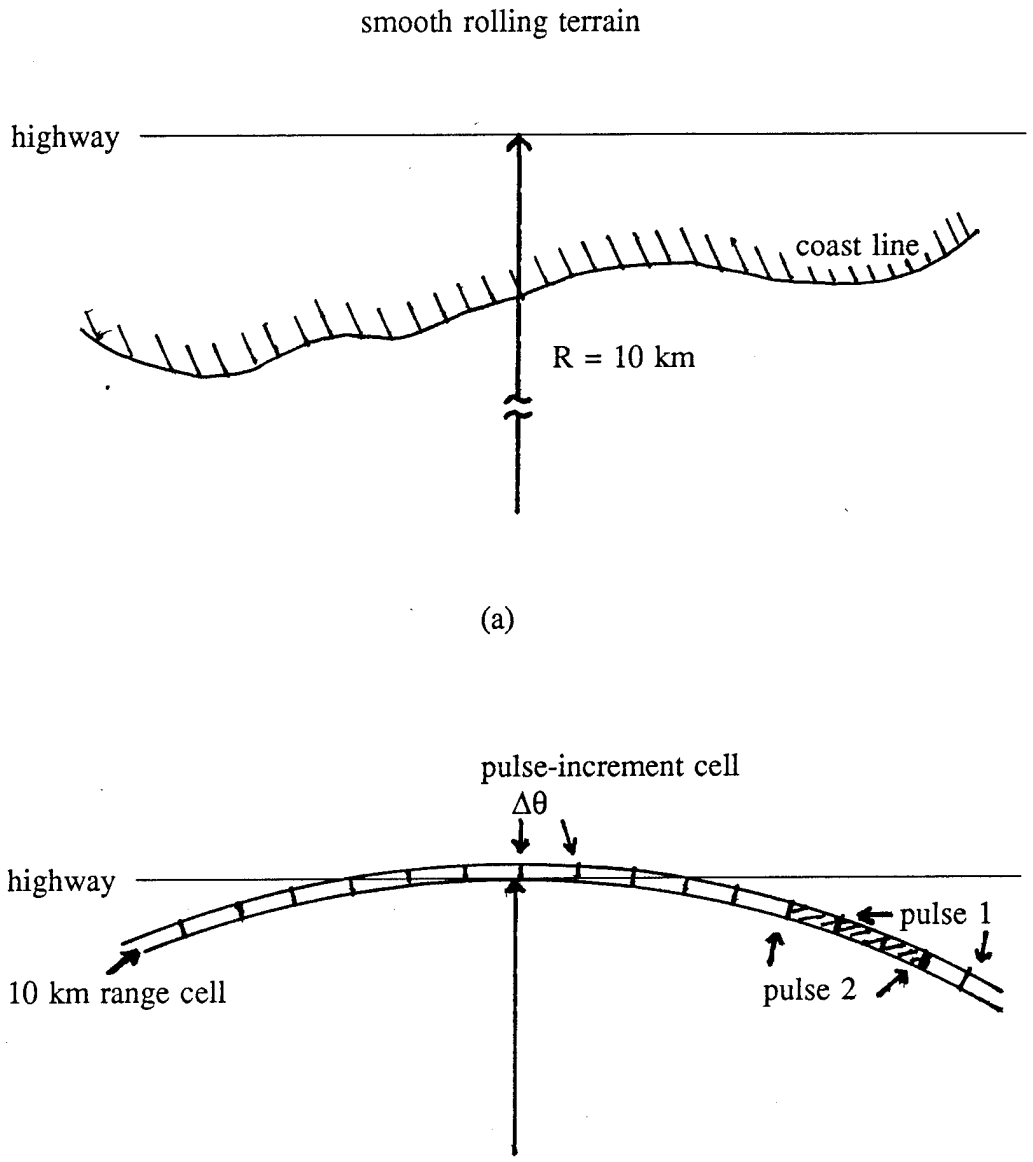

Figure 2. (a) A littoral environment; (b) pulse-increment cells for the synthesis of composite radar echo.

The radar antenna transmits its total output power into all directions. The radiated power is designed to fall off rapidly away from the mainbeam peak. For this study, only the echoes returning from the sector covered by the mainbeam will be considered. Specifically, a cutoff level of −30 dB is chosen because it makes no sense to include lower power levels of transmitted power when the sidelobes, which are radiating up to the −30 dB level, are ignored. Hence for this radar, the "footprint" contains 145 pulse-increment cells. The leading and the trailing edges of the footprint are at an $\theta_M = 5.22°$, corresponding to a gain level of about −30.13 dB below the peak. Note that the width of the footprint has been adjusted slightly upward so that it contains an integral number of pulse-increment cells. The antenna gain for each individual pulse-increment cell within the radar footprint is plotted in Figure 3.(a) while the mainbeam pattern is given in Figure 3.(b). The programs to determine the pertinent parameters and compute the gain levels are written in the Matlab* script language and included in Appendix A.

2. Pulse-Increment Composite Echo

Figure 2.(b) depicts the radar range cell at 10 km, extending over the 300 m depth to the 10.3 km range gate. Measured from the direction of the shortest distance from the radar, the angular sector from 13.86° to 19.37° of the next range cell (10.3 km to 10.6 km) contains the highway. The echoes from this 10.3 km range cell will be analyzed in this study.

As the radar scans through this angular sector of interest, the echoes will be the sum of the returns from the smoothly rolling terrain, which vary randomly in magnitudes and phases, and

---

* Matlab is a programming environment with strong numerical linear algebra and graphics support. It is adopted widely for instruction and research at the Naval Postgraduate School. The script language is close to FORTRAN. It is a product of The Math Works, Inc. of Natick, Mass.

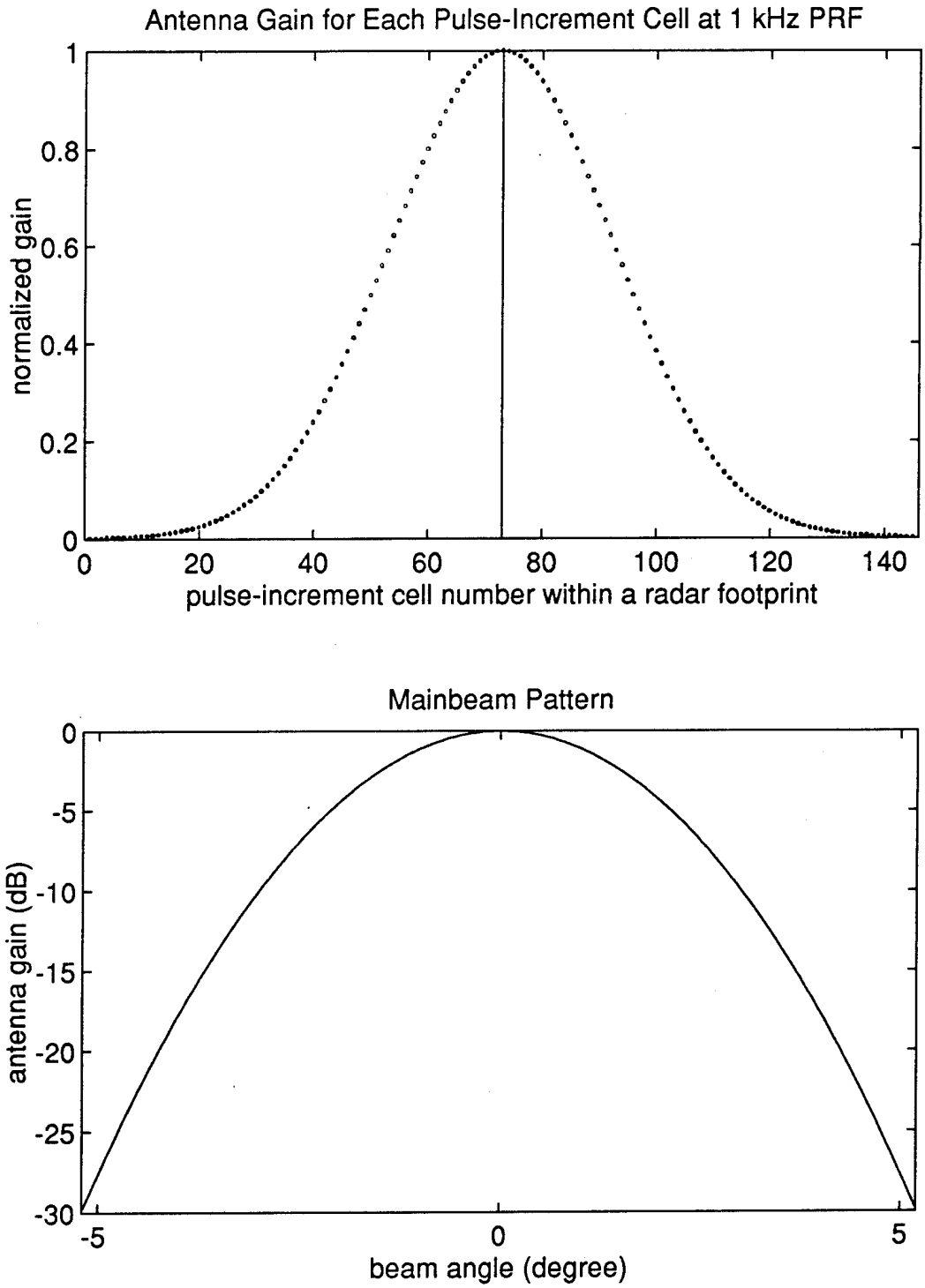

Figure 3. (a) Antenna gain for each pulse-increment cell at 1 kHz PRF. (b) Mainbeam pattern down to the −30 dB level below peak.

the returns from the highway, which change in magnitude and phase from a pulse-increment cell to another in a regular manner. Since the Doppler filters are linear and the returns from the random terrain do not contribute significantly to the output signals of the three channels of higher speed which are of interest, only the returns from the highway will be considered.

Assume that the radar scans in the counterclockwise direction as implied in Figure 2.(b) and the leading edge of its footprint is at 19.37° when a pulse is transmitted. At this instance, the mainbeam is pointing to the 24.59° direction, and the echo contains no return from the highway. One millisecond later, the next pulse is transmitted when the leading edge of the radar footprint covers the first pulse-increment cell. There are 76 more pulses transmitted before the leading edge of the beam encloses a pulse-increment cell which does not cover the highway. The trailing edge of the radar footprint leaves the last cell which covers the highway 145 pulses later when the mainbeam is pointing to the 8.64° direction. For the 221 pulses which contain echoes from the highway within the 10.3 to 10.6 km range, it is assumed that reflectivity of each pulse-increment cell, i.e., the strength of the echo from each cell, is proportional to the length of the highway in that cell. To each cell reflectivity, the phase shift due to path length delay is multiplied. The echo of each of these 221 pulses is composed by summing the reflectivity and phase-shift products of the cells covered by a pulse weighted by the antenna gain for each cell.

Moving windows of 6-pulse batches from the 221 plus one pulse before and one after them are fed into the Doppler filter bank batch by batch. The strengths of the output signals from each filter are plotted: Signals from filters 1, 0 and 5, centered at the Doppler velocities 27.76, 0 and −27.76 m/s respectively are presented in Figure 4. Signals from filters 2, 3 and 4, centered at the Doppler velocities 55.52, ±83.28 and −55.52 m/s respectively are presented in Figure 5.

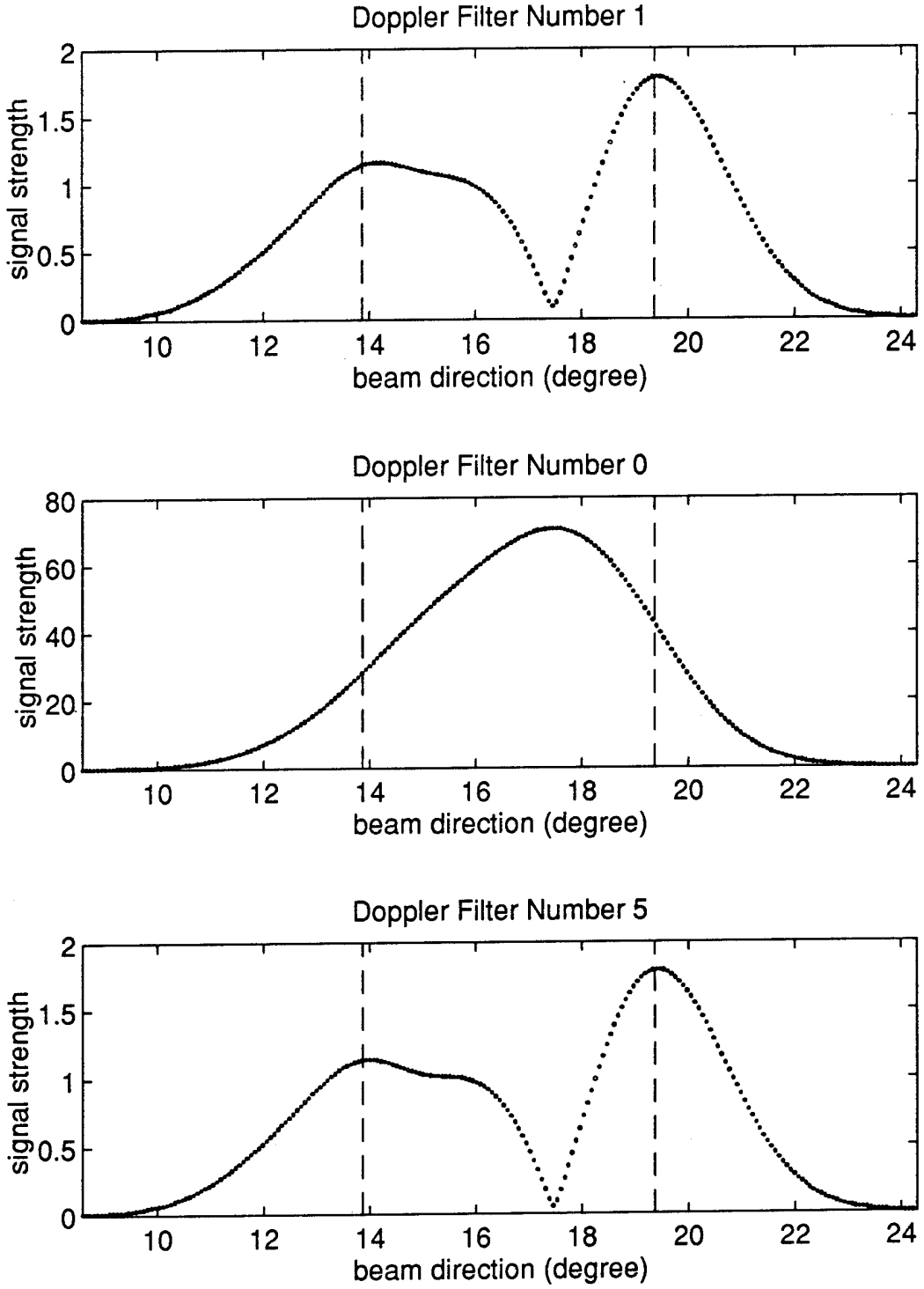

Figure 4. Output signal strength of channel 1, 0 and 5 of the Doppler filter bank as the radar scans over the extended object. The Doppler velocities at the centers of the channels are 27.76, 0 and −27.76 m/s respectively.

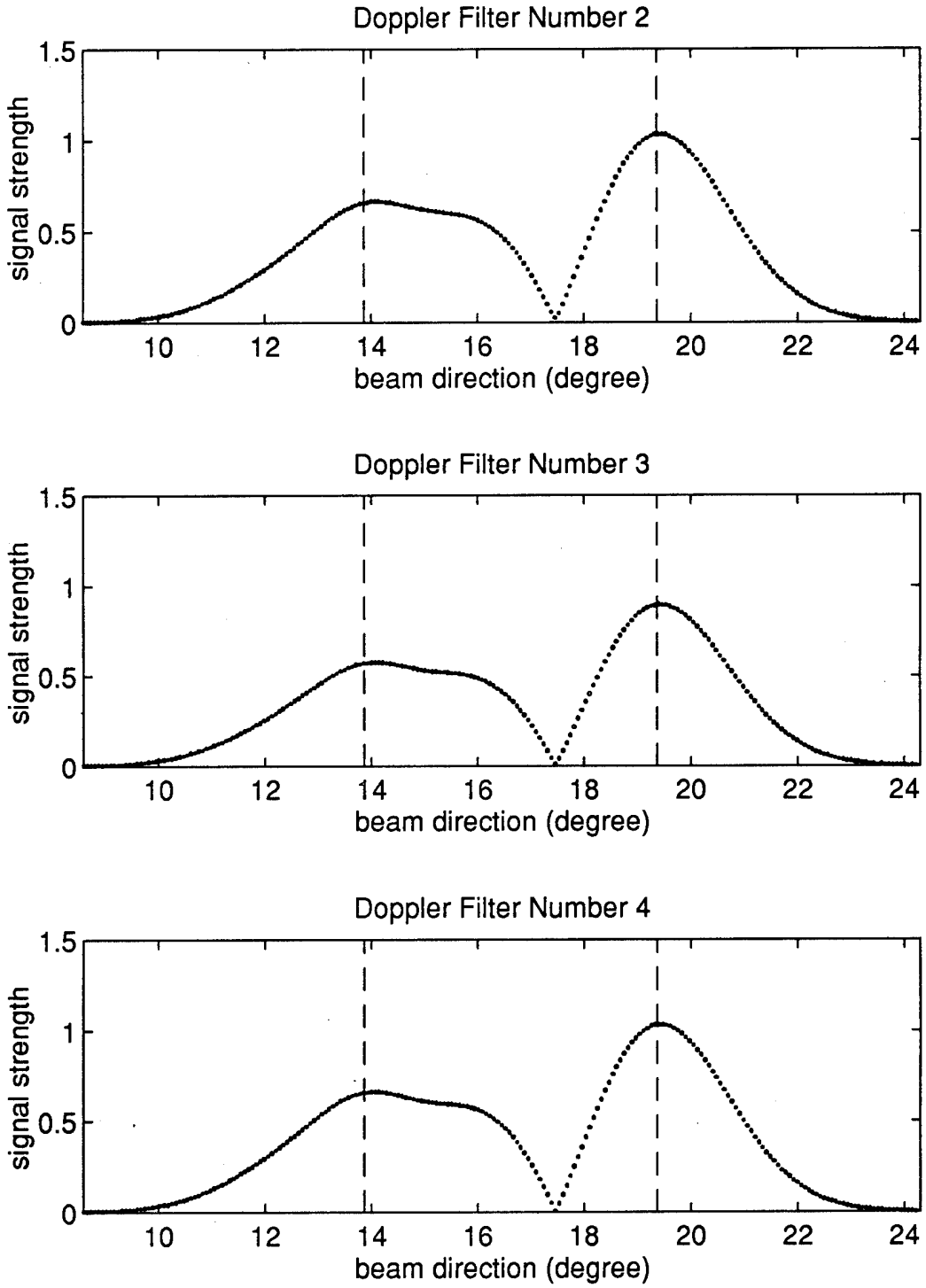

Figure 5. Output signal strength of channel 2, 3 and 4 of the Doppler filter bank as the radar scans over the extended object. The Doppler velocities at the centers of the channels are 55.52, ±83.28 and −55.52 m/s respectively.

The vertical dashed lines indicate the directions of the first and the last pulse-increment cells which contain the highway. The abscissae in Figures 4 and 5 give the mainbeam direction when the last of a batch of six pulses is transmitted. The Matlab programs implementing these procedures for constructing the radar echoes and carrying out the subsequent Doppler filtering are listed in Appendix B.

3. Velocity Estimation

The Doppler filters do not provide a direct reading of the apparent velocity of the extended object. To obtain an estimate, Ref. [2] suggests that the output signals from the three channels 2, 3 and 4, together called the moving channels, of the six-pulse Doppler filter be collapsed into one by selecting only the one of the greatest strength. The phases of two consecutive pulses are then compared to deduce the apparent velocity of the extended object. To avoid comparing output signals from two different channels to deduce the velocity, in this study the velocities from each channel are estimated separately before collapsing them into one. Note that the estimates are subject to the ambiguity of an integer multiples of 166.55 m/s. The estimated velocities are given in Figure 6.

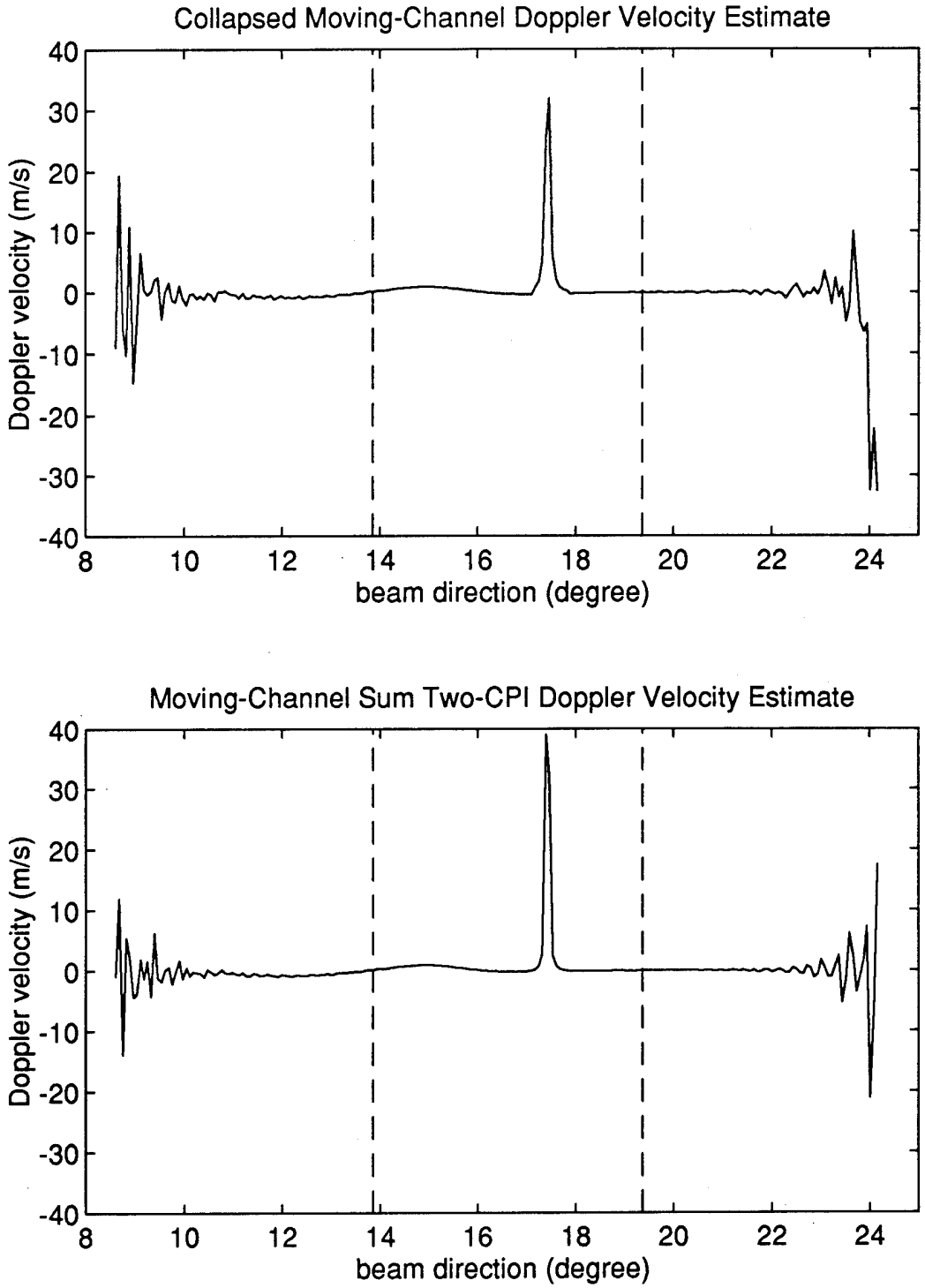

Figure 6. Apparent Doppler velocity of the extended object estimated using two different methods. The peak is 19 pulses wide from its base and is observed when the mainbeam is pointing to the 17.39° direction.

III. CONCLUSIONS

In this report, a technique to synthesize radar echo on a pulse-to-pulse basis is introduced. This technique can take advantage of digitized ground reflectivity data when such information about littoral regions becomes available.

The result of Chapter II confirms the assertion based on the arguments of Chapter I that the presence of extended objects which reflect radar power in a regular manner from pulse to pulse introduces phase shifts into the echoes which can impact the performance of the Doppler filters of a radar. Further studies are needed. In particular, it appears that the phenomenon is strongly system dependent, considering the fact that Figure 6 shows only a 19 ms spike when the radar beam with a Gaussian pattern scans over the section of highway in the 10.3 to 10.6 km range, in contrast to the prediction of Chapter I of the continuous presence of a Doppler phase shifted signal when a narrow but uniform radar beam is used.

It remains to be seen if specific techniques employed by different systems such as PRF stagger and frequency agility will be able to remove such false high speed targets efficiently. Furthermore, since this phenomenon is expected to occur when slow moving extended objects are present in short ranges, it is important to consider its impact on the proper deployment of weapon systems for ship self-defense.

APPENDIX A. ANTENNA GAIN FOR PULSE-INCREMENT CELLS

For a scanning antenna, from pulse to pulse the antenna mainbeam is pointing to a different direction. Therefore, antenna gain for each pulse-increment cell will also be different. Since a Doppler filter explores the pulse-to-pulse phase variation of the returned radar signal, to synthesize the pulse-increment composite echo, the antenna pattern must be digitized based on the pulse-increment cell size which depends on the pulse repetition frequency (PRF).

To model the mainbeam, a Gaussian pattern is assumed in this study. The pattern is covered down to -30 dB level below which sidelobes are assumed to be present. The mainbeam footprint therefore is limited to within $\pm\theta_M$, corresponding to the angles at which the gain drops to near the -30 dB level from beam maximum. The angular span of the radar footprint, $2\theta_M$, is chosen to be an integer multiple of $\Delta\theta$, the size of pulse-to-pulse angular increment of the beam. This is necessary so that the radar footprint will always cover an integral number of pulse-increment cells for the echo to be easily synthesized. On the other hand, by requiring an integral relationship between $\Delta\theta$ and θ_M, the leading edge of the radar footprint varies slightly for different PRF's in a multi-PRF system because $\Delta\theta$ changes with PRF.

In fact, if the whole antenna pattern is to be included so that the effects of sidelobes can be considered, for example, for the investigation of electronic countermeasures, the complete pattern must be digitized in increments of $\Delta\theta$, except maybe for the one interval containing the backward direction. This possibility should be allowed because 360 is unlikely, and may not even be desirable, to be an integer multiple of $\Delta\theta$ in degrees.

1. The CELLGAIN Function and Listing

The following Matlab M-file defines the function *cellgain* which computes the antenna gain for each pulse-increment cell within the radar footprint. Currently, only the mainbeam of the antenna is considered by setting the minimum gain level at the maximum sidelobe level. This function can be extended to include the complete antenna pattern in the future.

```
function [ncell,Dtheta,lead,gain] = cellgain(thetaB,gnmin,fscan,prf)
%cellgain
%  This function returns antenna mainbeam gain over each pulse-increment
%  cell within the radar footprint. A Gaussian beam pattern is assumed
%  with cutoff implemented at a prescribed dB level.
%  input: half-power beamwidth in degrees (thetaB), minimum gain level in
%     dB from peak to be considered (gnmin, must be negative), scanning
%     frequency in Hz (fscan), pulse repetition frequency in Hz (prf).
%  output: number of cells covered (ncell), cell angular size in degrees
%     (Dtheta), beam leading edge from center in degrees (lead), antenna
%     power gain over each pulse-increment cell in the radar footprint
%     (gain, vector of length ncell).
%
%  execution starts
%
Dtheta=360*fscan/prf;
lead=sqrt(-gnmin/40/log10(2))*thetaB;      %first estimate
ncell=ceil(2*lead/Dtheta);
nh=ncell/2;
lead=nh*Dtheta;
cell=1:ncell;
cell=cell-(nh+0.5);
gf=Dtheta/thetaB;
gf=-4*gf*gf;
gain=2.^((cell.*cell)*gf);
%
%  end of program
```

2. The Pattern Plotting M-File Listing and Output Diary

The Matlab M-file *antennav.m* calls the function *cellgain* and plots the resulted antenna gain for each pulse-increment cell and the mainbeam pattern as shown in Figure 3. The number of cells under the footprint, $\Delta\theta$, θ_M and the lowest power gain level are written to a diary file. The contents of the diary file are attached at the end of the program listing.

```
clear
thetaB=3.3;
sdlobe=-30;
fs=0.2;
prf=1000;                                   % PRI=1 ms
[ncell,Dth,thM,gain]=cellgain(thetaB,sdlobe,fs,prf);
save d:\matlab\vapparnt\antennad ncell prf fs thetaB Dth thM gain
centr=ncell/2+0.5;
glevel=thM/thetaB;
glevel=glevel*glevel*(-40*log10(2));
diary d:\matlab\vapparnt\antennad.dia
disp('      # cell     prf')
disp([ncell,prf])
disp('    Dtheta     thetaM')
disp([Dth,thM])
disp(' dB gain')
disp(glevel)
diary off
peakx=[centr,centr];
peaky=[0,1];
cell=1:ncell;
x1=0;
x2=ncell+1;
dbgain=10*log10(gain);
thetad=(cell-centr)*Dth;
thetai=floor(min(thetad)*10)/10;
thetaf=ceil(max(thetad)*10)/10;

figure(1)
```

```
set(gcf,'PaperOrientation','portrait',...
        'PaperPosition',[1,1.5,6.5,8.5]);

subplot(2,1,1)
plot(cell,gain,'.',peakx,peaky,'-')
axis([x1,x2,0,1])
xlabel('pulse-increment cell number within a radar footprint')
ylabel('normalized gain')
title('Antenna Gain for Each Pulse-Increment Cell at 1 kHz PRF')

subplot(2,1,2)
plot(thetad,dbgain,'-')
axis([thetai,thetaf,-30,0])
xlabel('beam angle (degree)')
ylabel('antenna gain (dB)')
title('Mainbeam Pattern')

clear
```

Diary output

```
      # cell       prf
      145          1000

      Dtheta       thetaM
      0.0720       5.2200

      dB gain
      -30.1289
```

3. Dependence of Pulse-Increment Cell on PRF

The following Matlab M-file *cellgplt.m* plots the antenna gain for each pulse-increment cell within the radar footprint. The Gaussian shaped mainbeam has a half-power beamwidth of 3.3°. Two pulse repetition frequencies at 850 Hz and 1170 Hz are considered, corresponding to the pulse repetition intervals of 1176.47 μs and 854.70 μs respectively. At 850 Hz, 123 pulse-increment cells of size $\Delta\theta = 0.0847°$ are allocated within the radar mainbeam. At the leading edge, $\theta_M = 5.2094°$, the gain level is -30.0068 dB below the mainbeam maximum. At 1170 Hz, 170 pulse-increment cells of size $\Delta\theta = 0.0615°$ are allocated. At the leading edge of the mainbeam, $\theta_M = 5.2308°$, the gain is -30.2533 dB below the maximum. These numbers are recorded in an output diary file attached to the end of this section. The antenna gain patterns for the pulse-increment cells are given in Figure A.1(a) and (b).

```
clear
thetaB=3.3;
sdlobe=-30;
fs=0.2;
prf1=850;                                   % PRI=1.17647 ms
prf2=1170;                                  % PRI=0.85470 ms
[ncl1,Dth1,thM1,gain1]=cellgain(thetaB,sdlobe,fs,prf1);
[ncl2,Dth2,thM2,gain2]=cellgain(thetaB,sdlobe,fs,prf2);
centr1=ncl1/2+0.5;
centr2=ncl2/2+0.5;
glevel=[thM1,thM2]/thetaB;
glevel=glevel.*glevel*(-40*log10(2));
diary d:\matlab\hm\cellgain.dia
disp('    # cell1      # cell2')
disp([ncl1,ncl2])
disp('    Dtheta1      Dtheta2')
disp([Dth1,Dth2])
disp('    lead1        lead2')
disp([thM1,thM2])
```

```
disp(' dB gain1    dB gain2')
disp(glevel)
diary off
peak1x=[centr1,centr1];
peak2x=[centr2,centr2];
peaky=[0,1];
cell1=1:ncl1;
cell2=1:ncl2;
x11=0;
x12=ncl1+1;
x21=0;
x22=ncl2+1;
figure(1)
set(gcf,'PaperOrientation','portrait',...
        'PaperPosition',[1,1.5,6.3,8.4]);
subplot(2,1,1)
plot(cell1,gain1,'.',peak1x,peaky,'-')
axis([x11,x12,0,1])
xlabel('pulse-increment cell number within a radar footprint')
ylabel('normalized gain')
title('Antenna Gain for Each Pulse-Increment Cell at 850 Hz PRF')
subplot(2,1,2)
plot(cell2,gain2,'.',peak2x,peaky,'-')
axis([x21,x22,0,1])
xlabel('pulse-increment cell number within a radar footprint')
ylabel('normalized gain')
title('Antenna Gain for Each Pulse-Increment Cell at 1170 Hz PRF')
clear
```

Diary output

```
      # cell1      # cell2
      123          170

      Dtheta1      Dtheta2
      0.0847       0.0615

      lead1        lead2
      5.2094       5.2308

      dB gain1     dB gain2
      -30.0068     -30.2533
```

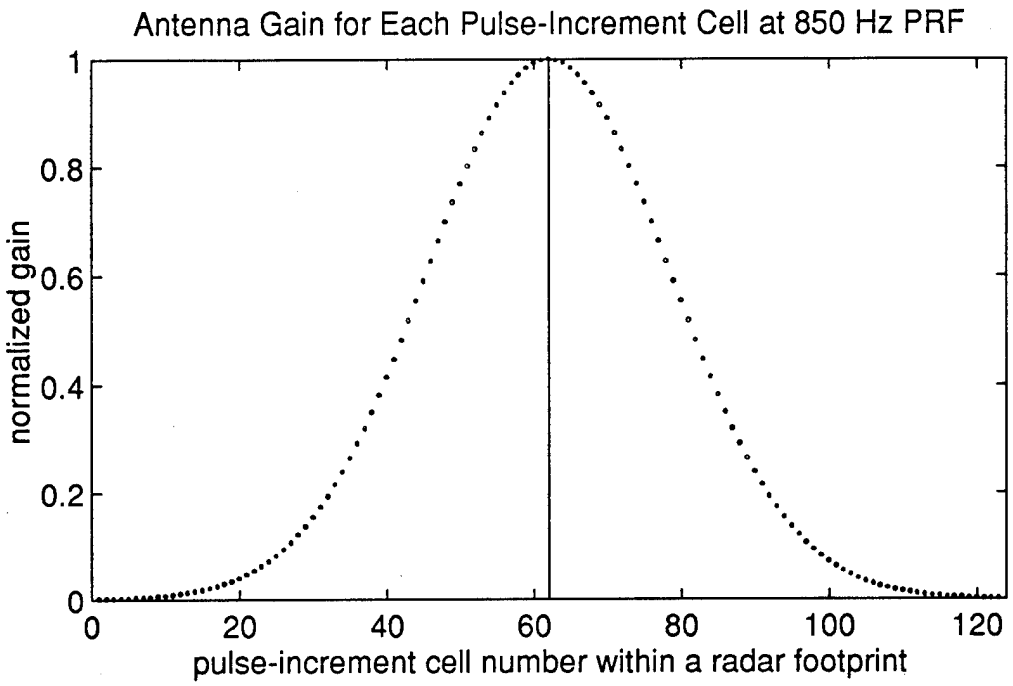

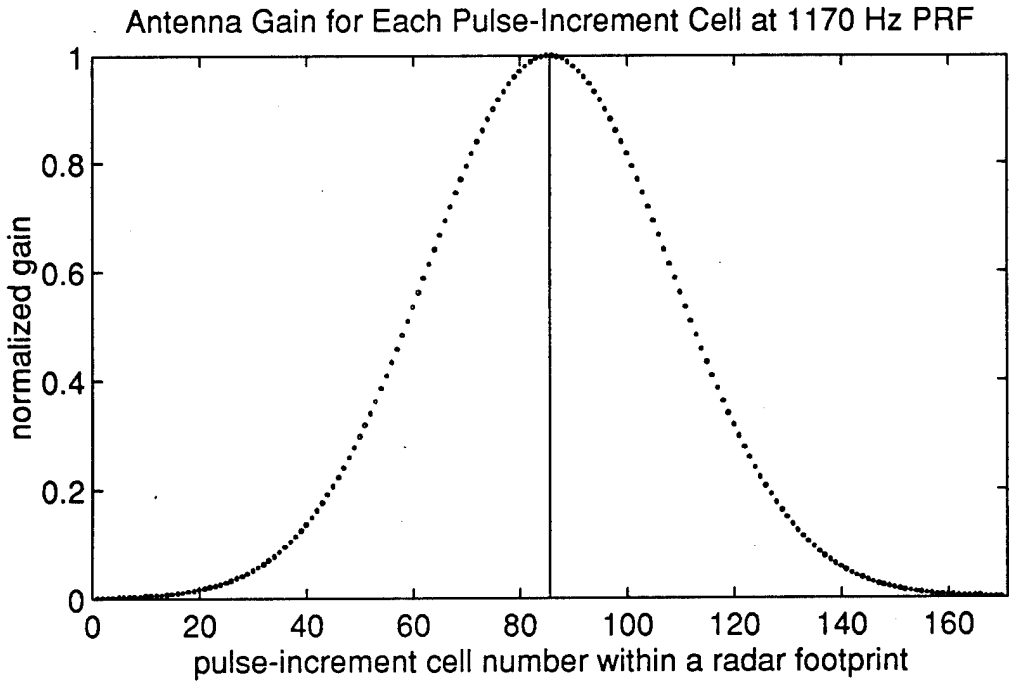

Figure A.1. Antenna gain for pulse-increment cells (a) at 850 Hz pulse repetition frequency; (b) at 1170 Hz pulse repetition frequency.

APPENDIX B. COMPOSITE ECHO AND DOPPLER FILTERING

The Matlab M-file *dopplerv.m* is written to synthesize the pulse-increment composite echoes returning from a straight stretch of highway in the 10.3 km range gate. The echoes are then fed through an FFT six-pulse Doppler filter. The output of each filter is plotted using the M-file *dplrvplt.m.*

1. The DOPPLERV.M M-File Listing

```
%dopplerv.m
%
% In this program, the composite echoes are synthesized and their
% output from a 6-pulse Doppler filter are computed.
%
%  radar parameters:
%     operating frequency: 900 MHz
%     PRF: 1000 Hz
%     number of pulse integrated (ncpi) for Doppler processing: 6
%           ambiguous velocity: 166.55 m/s
%           velocity at the center of a filter:
%              #0: 0; #1: 27.76 m/s; #2: 55.52 m/s; #3: 83.28 m/s;
%              #4: -55.52 m/s; #5: -27.76 m/s
%
%  description of extended object in the 10.3 km range cell:
%     A straight section of highway is in this range cell extending
%     from theta1 = arccos(1/1.03) to theta2 = arccos(1/1.06), measured
%     from the direction of the shortest distance from the radar. This
%     direction of shortest distance will be taken as the reference
%     direction. The distance to the extended object along this direction
%     is 10 km.
%
%  beam scanning assumption:
%     At t = 0, the leading edge of the mainbeam coincides with theta1
%     and is moving toward theta2. The mainbeam direction at t = 0 is
%     denoted as theta0. The angle will be decreasing as the radar scans
%     towards the reference direction.
%
%The following steps are taken to compute the apparent velocity of
%the stationary extended object:
%  1. Determine the pulse-increment cell size and subdivide the
%     radar mainbeam accordingly.
%  2. Assign pulse-increment cells to the extended object and
%     determine the phase delays of echoes from individual cell.
%     The fraction of the object in the last pulse-increment cell
%     is also estimated.
%  3. Synthesize the radar echoes as the mainbeam scans over the
%     extended object.
```

```
%  4. Invoke Doppler processing to determine the response in each
%     filter while the radar is scanning.
%
clear
%
%  define radar parameters
%
lcwave=299792458/9e8;                    % fc = 900 MHz
ncpi=6;
%
%  Step 1.
%
% save d:\matlab\vapparnt\antennad ncell prf fs thetaB Dth thM gain
load d:\matlab\vapparnt\antennad
%
%  Step 2.
%
pi2=2*pi;
rd2dg=180/pi;
dg2rd=pi/180;
range=10300;                     % range cell in meters
range2=2*range;
Dthrad=Dth*dg2rd;
theta1=acos(1/1.06);
theta2=acos(1/1.03);
theta0=theta1*rd2dg+thM;         % mainbeam direction at t = 0
fnd103=(theta1-theta2)/Dthrad;
nclobj=ceil(fnd103);
fnd103=fnd103+1-nclobj;          % fraction of object in the last cell
r10300=1:nclobj;
r10300=r10300-0.5;               % reference to mid-point of the cell
r10300(nclobj)=r10300(nclobj)-0.5+fnd103/2;
r10300=theta1-Dthrad*r10300;
r10300=(range2-range2./cos(r10300))/lcwave;
r10300=(r10300-floor(r10300))*pi2;      % remove integer multiples of 2*pi
reflec=exp(j*r10300);
reflec(nclobj)=fnd103*reflec(nclobj);
%
%  Step 3.
%
ncell1=ncell-1;
```

```
rbeam=zeros(1,ncell1)+j*zeros(1,ncell1);
rscan=[rbeam,reflec,rbeam];
necho1=ncell+nclobj;
nechos=necho1+1;
echoes=zeros(1,nechos);
%  step the beam through the object
   for npulse=2:necho1;
ntrail=npulse-1;
nlead=ntrail+ncell1;
echoes(npulse)=rscan(ntrail:nlead)*gain';
   end
%
%  Step 4.
%
ncp1=ncpi-1;
ndelay=nechos-ncp1;
edelay=zeros(ncpi,ndelay);
   for npulse=1:ndelay;
np2=npulse+ncp1;
etemp=echoes(npulse:np2);
edelay(:,npulse)=etemp';
   end
vdf=fft(edelay);
vf0=vdf(1,:);
vf1=vdf(2,:);
vf2=vdf(3,:);
vf3=vdf(4,:);
vf4=vdf(5,:);
vf5=vdf(6,:);
%
%  save output
%
t=ncp1:necho1;
thetat=theta0-Dth*t;
th1=theta1*rd2dg;
th2=theta2*rd2dg;
save d:\matlab\vapparnt\dopplerv lcwave prf th1 th2 thetat...
                                 vf0 vf1 vf2 vf3 vf4 vf5
%
clear
```

2. The Plotting Routine DPLRVPLT.M M-File Listing

```
%dplrvplt.m
%
%This program plots the 6-pulse Doppler filter output computed with
%dopplerv.m and saved in the file dopplerv.mat.
%
%save d:\matlab\vapparnt\dopplerv lcwave prf th1 th2 thetat vf0 vf1 vf2 vf3
vf4 vf5
%
load d:\matlab\vapparnt\dopplerv
vd0=abs(vf0);
vd1=abs(vf1);
vd2=abs(vf2);
vd3=abs(vf3);
vd4=abs(vf4);
vd5=abs(vf5);
%
line1=[th1,th1];
line2=[th2,th2];
leng0=[0,80];
leng1=[0,2];
leng3=[0,1.5];
thini=(floor(min(thetat)*10)/10);
thfin=(ceil(max(thetat)*10)/10);
%
figure(1)
%
set(gcf,'PaperOrientation','portrait',...
        'PaperPosition',[1,1.5,6.5,8.5]);
%
subplot(3,1,1)
plot(thetat,vd1,'.',line1,leng1,'--',line2,leng1,'--')
axis([thini thfin 0 2]);
xlabel('beam direction (degree)')
ylabel('signal strength')
title('Doppler Filter Number 1')
%
subplot(3,1,2)
plot(thetat,vd0,'.',line1,leng0,'--',line2,leng0,'--')
```

```
axis([thini thfin 0 80]);
xlabel('beam direction (degree)')
ylabel('signal strength')
title('Doppler Filter Number 0')
%
subplot(3,1,3)
plot(thetat,vd5,'.',line1,leng1,'--',line2,leng1,'--')
axis([thini thfin 0 2]);
xlabel('beam direction (degree)')
ylabel('signal strength')
title('Doppler Filter Number 5')
%
figure(2)
%
set(gcf,'PaperOrientation','portrait',...
        'PaperPosition',[1,1.5,6.5,8.5]);
%
subplot(3,1,1)
plot(thetat,vd2,'.',line1,leng3,'--',line2,leng3,'--')
axis([thini thfin 0 1.5]);
xlabel('beam direction (degree)')
ylabel('signal strength')
title('Doppler Filter Number 2')
%
subplot(3,1,2)
plot(thetat,vd3,'.',line1,leng3,'--',line2,leng3,'--')
axis([thini thfin 0 1.5]);
xlabel('beam direction (degree)')
ylabel('signal strength')
title('Doppler Filter Number 3')
%
subplot(3,1,3)
plot(thetat,vd4,'.',line1,leng3,'--',line2,leng3,'--')
axis([thini thfin 0 1.5]);
xlabel('beam direction (degree)')
ylabel('signal strength')
title('Doppler Filter Number 4')
%
clear
```

APPENDIX C. THE VELOCITY ESTIMATION ROUTINE

Signals from the three higher speed channels of the six-pulse FFT Doppler filter are utilized to deduce the apparent Doppler velocity. The phases of two consecutive pulses from the higher speed channels 2, 3 and 4 are compared to deduce the apparent velocity of the extended object. The results are then collapsed into one by selecting only the velocity deduced from the signals of the greatest strength [2]. Another approach is to sum the signals from the three channels coherently to form a pulse and compare the phases of two consecutive such pulses. These procedures are carried out with the Matlab M-file *vestm.m* listed below. The results are plotted in Figure 6.

1. The Velocity Estimating Routine VESTM.M M-File Listing and Output Diary

```
%vestm.m
%
%This program computes target velocity using the moving channel output
%of the 6-pulse Doppler filter of dopplerv.m.
%
%save d:\matlab\vapparnt\dopplerv lcwave prf th1 th2 thetat
%                                 vf0 vf1 vf2 vf3 vf4 vf5
%
load d:\matlab\vapparnt\dopplerv
clear vf0 vf1 vf5
%
ndata=length(thetat);
ndata1=ndata-1;
angles=thetat(2:ndata);
%
% velocity estimate from channels 2, 3 and 4
%
vm1=vf2(1:ndata1);
vm2=vf2(2:ndata);
vphase=angle(vm2./vm1);
vmove2=(lcwave*prf/4/pi)*vphase;
%
vm1=[];
vm2=[];
vphase=[];
vm1=vf3(1:ndata1);
vm2=vf3(2:ndata);
vphase=angle(vm2./vm1);
vmove3=(lcwave*prf/4/pi)*vphase;
%
vm1=[];
vm2=[];
vphase=[];
vm1=vf4(1:ndata1);
vm2=vf4(2:ndata);
vphase=angle(vm2./vm1);
vmove4=(lcwave*prf/4/pi)*vphase;
%
```

```
%  select the strongest filter output from the three moving channels
%
vEstm=zeros(1,ndata1);
iold=2;
   for idata=1:ndata1
idata1=idata+1;
vf=[vf2(idata1);vf3(idata1);vf4(idata1)];
vest=[vmove2(idata);vmove3(idata);vmove4(idata)];
vmag=abs(vf);
[vmagx,I]=max(vmag);
      if vmagx > vmag(iold)
vEstm(idata)=vest(I(1));
iold=I(1);
      else
vEstm(idata)=vest(iold);
      end
   end
%
vmoves=vf2+vf3+vf4;
vms1=vmoves(1:ndata1);
vms2=vmoves(2:ndata);
vphass=angle(vms2./vms1);
vEsts=(lcwave*prf/4/pi)*vphass;
%
[vmax,I]=max(vEsts);
tmax=I(1);
thmax=angles(I(1));
I1=tmax;
I2=I1-1;
   while vEsts(I2) < vEsts(I1)
I1=I2;
I2=I1-1;
   end
t1=I1;
vest1=vEsts(I1);
angle1=angles(I1);
I1=max(I);
I2=I1+1;
   while vEsts(I2) < vEsts(I1)
I1=I2;
I2=I1+1;
```

```
   end
t2=I1;
vest2=vEsts(I1);
angle2=angles(I1);
%
diary d:\matlab\vapparnt\vestm.dia
disp('   vEst1   vmax    vEst2')
disp([vest1,vmax,vest2])
disp('   angle1  thmax   angle2')
disp([angle1,thmax,angle2])
disp('   t1      tmax     t2')
disp([t1,tmax,t2])
diary off
%
%
save d:\matlab\vapparnt\vestm angles vEstm vEsts
%
figure(1)
%
angl1=floor(min(angles));
angl2=ceil(max(angles));
line1=[th1,th1];
line2=[th2,th2];
high0=[-40,40];
%
set(gcf,'PaperOrientation','portrait',...
        'PaperPosition',[1,1.5,6.5,8.5]);
%
subplot(2,1,1)
%
plot(angles,vEstm,'-',line1,high0,'--',line2,high0,'--')
axis([angl1,angl2,-40,40])
xlabel('beam direction (degree)')
ylabel('Doppler velocity (m/s)')
title('Collapsed Moving-Channel Doppler Velocity Estimate')
%
subplot(2,1,2)
%
plot(angles,vEsts,'-',line1,high0,'--',line2,high0,'--')
axis([angl1,angl2,-40,40])
xlabel('beam direction (degree)')
```

```
ylabel('Doppler velocity (m/s)')
title('Moving-Channel Sum Two-CPI Doppler Velocity Estimate')
%
clear
```

Diary output

```
      vEst1        vmax         vEst2
      -0.0907      39.1078      -0.2246

      angle1       thmax        angle2
      18.1100      17.3900      16.7420

      t1           tmax         t2
      85           95           104
```

BIBLIOGRAPHY

1. *Radar Handbook*, 2nd ed., M. I. Skolnik, editor, McGraw-Hill, New York, 1990.

2. *Prime Item Function Specification for the Long Range Air Surveillance Radar AN/SPS-49A(V)1*, Naval Sea Systems Command, 15 September 1994.

INITIAL DISTRIBUTION LIST

	No. Copies
1. Defense Technical Information Center Cameron Station Alexandria, VA 22304-6145	2
2. Dudley Knox Library Code 52 Naval Postgraduate School Monterey, CA 93943-5101	2
3. Chairman, Code EC Department of Electrical and Computer Engineering Naval Postgraduate School Monterey, CA 93943-5121	1
4. Hung-Mou Lee, EC/Lh Department of Electrical and Computer Engineering Naval Postgraduate School Monterey, CA 93943-5121	2
5. Program Executive Office, Ship Defense Attn: Mr. George Hamilton (TAD)-D1 NC 2, Room 8E68 2531 Jefferson Davis Highway Arlington, VA 22242-5170	1